Methods for Assessing the Bearing Capacity of Offshore Pile Based on Field Tests Conducted in the Persian Gulf

Haghighat Mahdiyan[2], Bahram Nadi[3], Mahmood Vafaeian[1]

1-Full professor,Department of Civil Engineering, Najafabad Branch, Islamic Azad University, Najafabad, Iran

2-PhD Student,Department of Civil Engineering, Najafabad Branch, Islamic Azad University, Najafabad, Iran

3- Assistant Professor , Department of Civil Engineering, Najafabad Branch, Islamic Azad University, Najafabad, Iran

Abstract

Long steel piles pushed into the seabed are the most typical foundation type for fixed offshore structures. Selecting the right dimensions for the piles and guaranteeing the stability of the platform depend on precisely calculating their bearing capacity. The in-situ cone penetration test has gained a lot of popularity as a bearing capacity estimation tool for offshore piles in recent years. Its benefits include accurate results and continuous data recording at depth, among others. Using data collected from field tests in the South Pars region, this research calculates the axial bearing capacity of steel piles utilized as foundations in Persian Gulf offshore platforms. This is achieved by first presenting analytical-experimental equations grounded on the CPT test findings and subsequently calibrating them using the data from the dynamic pile test. Lastly, the geometric properties of the piles and the ideal penetration depth are determined using these created equations in conjunction with gene expression programming. The results demonstrated that the offered method could ascertain the ideal geometric properties of offshore-driven piles in the Persian Gulf area in both cohesive and non-cohesive soils.

Keywords: Cone penetration test; Offshore pile foundation; Axial bearing capacity; Dynamic pile test.

1. Introduction

The majority of offshore constructions in shallow waters, such the Persian Gulf, are fixed jacket platforms. Pile foundations are typically used to support and secure these structures, which are fabricated from tubular steel components [1,2]. The features of the soil on the seabed are unknown, and offshore platforms operate in hostile environments. Therefore, it is critical to ensure that the foundations of large structures are both economically and safely designed in order to keep them stable under different loads and to lessen the financial, environmental, and human casualties that would result from the structure's collapse. Offshore jacket platforms supported by piles are susceptible to scouring, soil liquefaction, and pile bearing capacity and lateral behavior, among other factors [3,4,5]. To account for the fact that soil properties can vary depending on where the structure is being installed, it is necessary to have equations that can be used to estimate the geometric properties and penetration depth of the piles. This will guarantee that the structure is sufficiently safe and keep the design from becoming uneconomical [5,6].

In order to evaluate and estimate the bearing capacity of steel-driven friction piles, numerous formulae have been developed during the last several decades. Nevertheless, uncertainties arise from the complexity of the soil environment when applying these equations in varied contexts. The bearing capacity of piles can be determined using a variety of methods now in use, including as static analysis, dynamic testing, static pile load testing, and in-situ testing [7]. The most comprehensive and precise way to anticipate in-place pile bearing capacity is the static pile load test, which takes into account the site's real conditions to establish its value. On the other hand, this approach is laborious and complicated, particularly for offshore projects [8]. One way to evaluate a pile dynamically is to use a Pile Driving Analyzer (PDA) to track the acceleration and strain close to the pile head as you drive. Estimates of ultimate pile bearing capacity, pile driving stresses, and energy transfer are all computed using these observations [9]. When assessing the reliability of static analysis and in-situ testing methods for estimating pile bearing capacity, the dynamic analysis of the pile loading test is typically utilized as a criterion.

Different results are obtained when the bearing capacity of piles is assessed using static analytical methods. For this reason, techniques that rely on in-situ testing like the cone penetration test (CPT), the standard penetration test (SPT), the pressure meter test (PMT), and others have been proposed to improve the precision of the calculated values [10,11]. As a result of their many benefits, including fast testing times, high accuracy and repeatability, and the ability to extract attachment information from soil stratification, CPT and CPTu procedures have recently replaced other field tests as the gold standard for determining piles' axial bearing capacity [12]. These techniques are seen as supplementary or even replacements for static analysis methods. Data from CPT or CPTu has an advantage over theoretical model analysis when it comes to pile design since it eliminates the need for undisturbed sampling and subsequent laboratory tests during the design process [13].

Pile carrying capacity determination utilizing CPT test results with various soil conditions has been the subject of substantial research over the last several decades. The research resulted in the presenting of equations that took soil properties and other elements into account [14–19]. Taking

into account the many approaches offered to calculate pile carrying capacities from CPT data, Muoshfeqhi and Eslami [20] assess the current approaches by analyzing data collected from 47 sources across 23 nations, with the majority of these sources headquartered in the US. Among the diverse soil types included in this database are clayey soils (42%), sandy soils (35%), and mixed soils (23%).

The findings indicate that evaluations in soils with diverse properties are required for the optimal design of piles using the suggested equations. When designing the offshore pile, these assessments are of utmost importance. Given the CPT method's reliability in providing soil properties, approaches that correlate CPT data with pile bearing capacity have demonstrated to have improved accuracy in pile design: [21]. Pile bearing capacity estimation in the Persian Gulf based on CPT in-situ test findings has received little attention from researchers. In this study, an analytical and experimental equation based on CPT tests was proposed using data from case studies in the South Pars region. The equation was tested and calibrated using results from previous PDA. Lastly, the ideal dimensions of the pile design were determined based on the site soil characteristics. An artificial intelligence system based on gene expression programming (GEP) was used to determine the correlation and relative relationship between the CPT data and the pile bearing capacity.

2. Materials and Methodology

This research determined the ultimate bearing capacity of the pile by first using in-situ test results from CPTs performed on soils with different properties in the studied offshore area of the Persian Gulf. Then, they used the American Petroleum Institute's (API) proposed modified approach [22] to calculate the bearing capacity. Next, the current dynamic tests are utilized to calibrate the relationship between the CPT results and the pile's bearing capacity. Then, a more accurate correlation between the two is expressed using the gene expression programming technique. The best pile dimensions are then estimated using this smart computational approach and the CPT results. Here we will go over each of these steps.

2.1. Research Location and Site Evaluation Details

On the eastern end of the sea border between Iran and Qatar lies the examined area, which is situated in the 17th and 18th phases of the South Pars region. Wellhead offshore jacket platforms, developed and built by Iran Offshore Engineering and Construction Company (IOEC), have increased exploitation capacity and opened up new energy extraction fields. Dataset utilized in this study is derived from geotechnical investigations and testing performed for the purpose of designing and installing SPD 23 and 24 platforms (refer to Fig. 1).

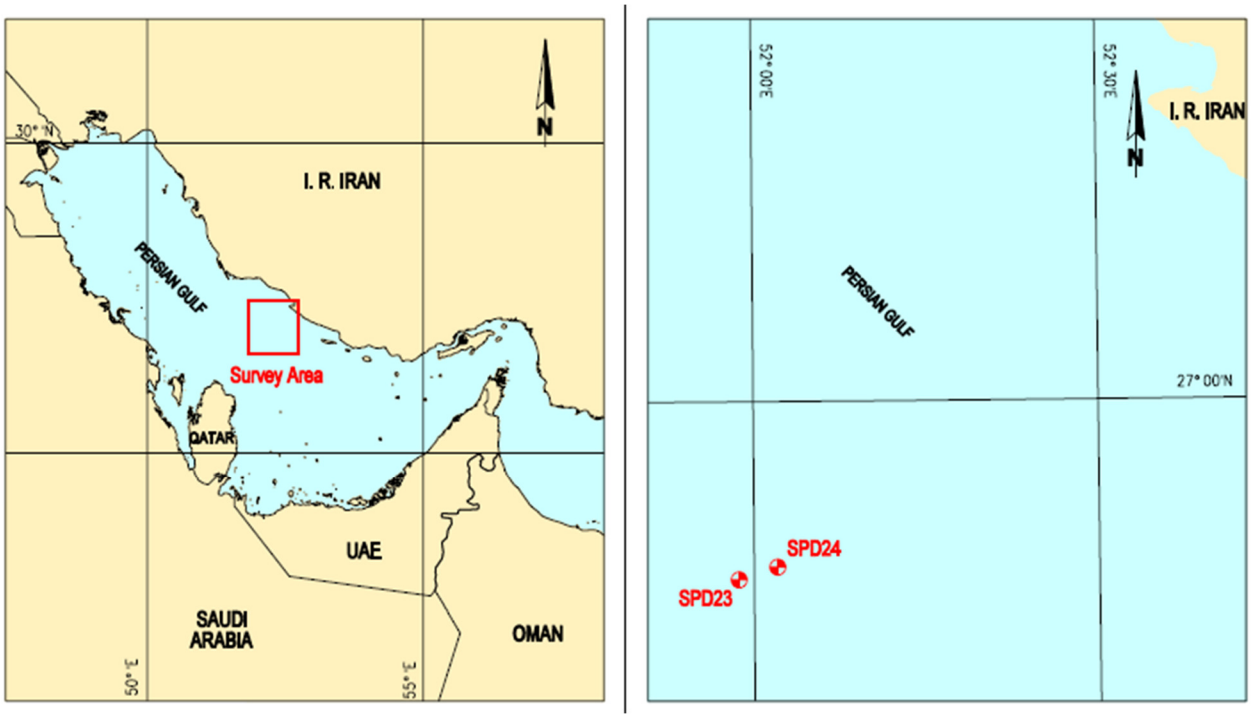

Fig. 1 The location of boreholes

2.2. Cone Penetration Test Method

With its high output rate, repeatability of data, and near-continuous profiling of geotechnical parameters, Cone Penetration Testing is an in-situ test that is often and usefully employed for geotechnical site studies. Another useful tool for determining the depth of the foundation is the visual representation of the CPT result. Subsurface conditions at the test site are properly indicated by it [23]. A cone penetrometer is driven into the ground at a constant velocity in this test, and electronic readings are taken at predetermined intervals. A steel cone is driven vertically into the earth using a cone penetration test apparatus. As a cone is penetrating, the cone penetration meter records the resistance of the tip and friction sleeve.

International Society for Soil Mechanics and Geotechnical Engineering (ISSMGE) produced a reference test protocol, which the test technique follows [24]. The CPT test yielded the example findings shown in Fig. 2.

Test for Pile Driving Analyzer 2.3

A high strain dynamic pile test is the pile driving analyzer testing. Testing the load-bearing capability of a pile while the hummer is operating on it is a quick, accurate, and inexpensive process. The CASE Method, which stands for Stress Wave Propagation on Piles, is the theoretical foundation of this test. You can find out about the pile's activated bearing capacity, hammer performance, maximum driving stresses, and integrity by measuring the force (strain) and velocity (acceleration) signals. These sensors are attached to the pile and performed near the top of the pile during impact. Next, the data was subjected to a more thorough evaluation using

the CAPWAP (Case Pile Wave Analysis Program) software, which is known for its rigorous numerical analysis [25-27].

Before the CAPWAP program can determine the pile carrying capacity using the data collected from the PDA, it must receive the speed curve recorded by the PDA for each soil element. After that, it takes the soil properties, like damping and rupture displacement, at face value. The software then determines the force wave curve at the pile head by utilizing the data that has been received, which includes the pile's internal movements (the velocity curve at the pile head) and the assumptions about the boundary conditions (modelling parameters for the soil). Following the determination of the pile top force, the computed curve is contrasted with the curve derived from the PDA device. When the two curves don't line up, engineers and experts in the field will make adjustments to the soil parameters and recalculate the force wave curve. When the predicted and observed force curves agree well, the procedure is repeated [25–27]. The CAPWAP results for FSP 24 are displayed in Fig. 3.

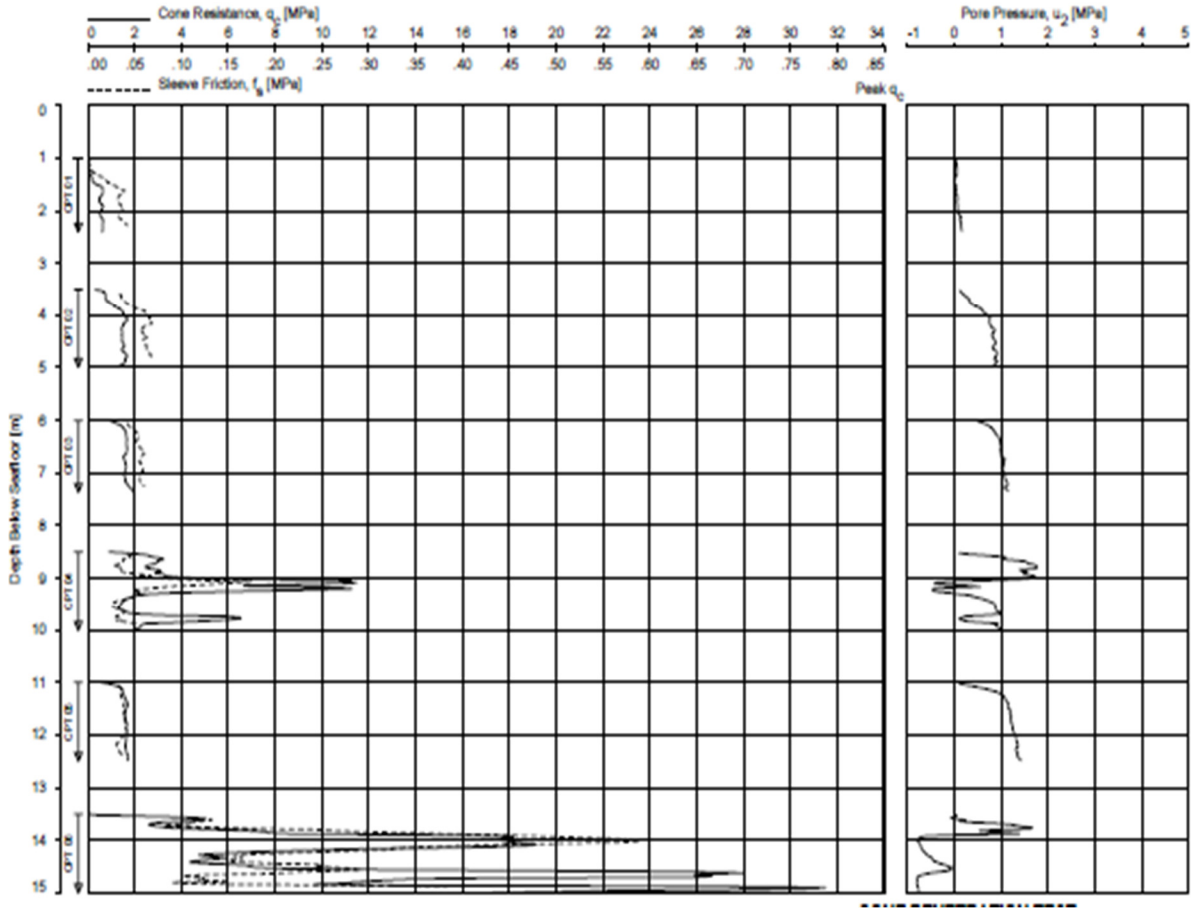

Fig. 2 Cone penetration test of SPD23

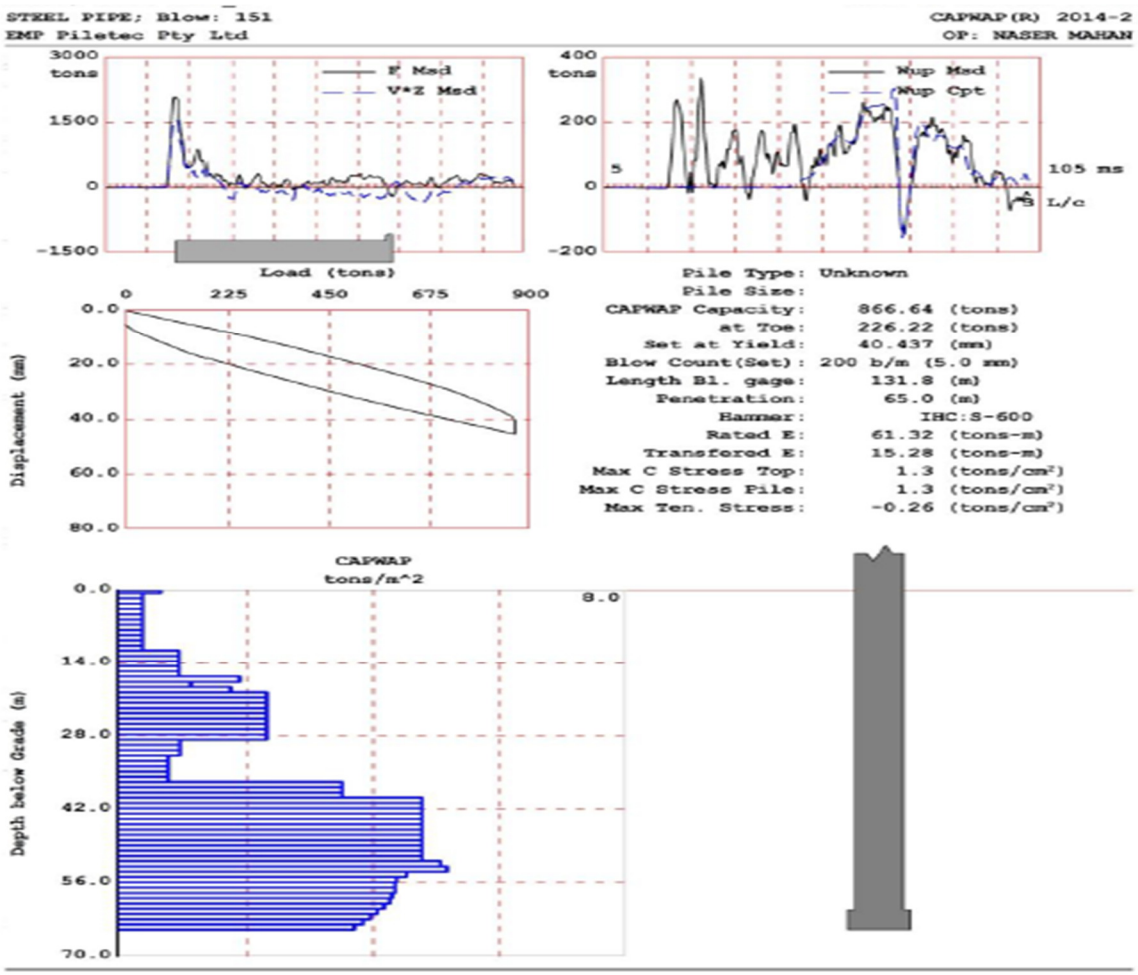

Fig. 3 Results obtained from CAPWAP for FSP24

2.4. Data Sets

A database was prepared using data from 43 operations of driving closed steel pipe piles in the studied area. The goal was to develop models using computational intelligence algorithms that could determine the correlation and relationship between in-situ test results and pile bearing capacity. Table 1 displays the results of the CPT for cohesive and non-cohesive soils, which include the strength of the pile tip and skin friction (q_c and f_s, respectively), as well as the ultimate bearing capacity (Q_u) of the pile. The database also has information about the type of soil and the geometrical characteristics of the pile, such as its length (L) and diameter (D).

Table 1. Database collection

NUM	depth	soil type	f_s(MN/m)	f_s(Mpa)	q_s(MN)	q_s(MPa)	L	D(m)	Q_u(MN)
1	39.2	silt	0.072	0.015046	3.15	1.72771	39.2	1.524	14.329
2	40.1	silt	0.37	0.077319	2.46	1.34926	40.1	1.524	13.983
3	45	clay	0.43	0.089857	2.87	1.574136	45	1.524	16.872
4	67.2	silt	0.565	0.118068	3.28	1.799013	67.2	1.524	33.859
5	72	clay	0.616	0.128726	3.61	1.980011	72	1.524	38.367
6	84	sand	0.072	0.015046	3.32	1.820952	84	1.524	49.23
7	84.5	clay	0.642	0.134159	3.28	1.799013	84.5	1.524	49.461
8	96	silt	0.67	0.14001	3.28	1.799013	96	1.524	61.248
9	100.5	silt	0.67	0.14001	5.62	3.082455	100.5	1.524	67.719
10	103.8	clay	0.802	0.167594	4.1	2.248766	103.8	1.524	67.026
11	110.5	clay	0.827	0.172819	4.1	2.248766	110.5	1.524	73.729
12	40.4	silt	0.057	0.014892	2.18	1.868871	40.4	1.219	10.917
13	41	clay	0.332	0.086737	1.89	1.62026	41	1.219	11.041
14	66	clay	0.445	0.116259	2.1	1.800289	66	1.219	25.141
15	80.5	clay	0.554	0.144736	2.61	2.237502	80.5	1.219	35.524
16	40.4	silt	0.043	0.014983	1.28	1.951857	40.4	0.914	6.581
17	41	clay	0.249	0.086761	1.06	1.616381	41	0.914	6.684
18	66	clay	0.335	0.116726	1.18	1.799368	66	0.914	15.424
19	80.5	clay	0.415	0.144601	1.47	2.241585	80.5	0.914	21.697
20	40.1	sand	0.057	0.014892	1.92	1.645979	40.1	1.219	11.2
21	41.7	clay	0.33	0.086215	1.89	1.62026	41.7	1.219	11.323
22	65	clay	0.438	0.11443	2.1	1.800289	65	1.219	24.492
23	80.5	clay	0.55	0.143691	2.61	2.237502	80.5	1.219	35.323
24	40.1	sand	0.043	0.014983	1.08	1.646879	40.1	0.914	8
25	41.7	clay	0.247	0.086064	1.06	1.616381	41.7	0.914	8.123
26	65	clay	0.329	0.114636	1.18	1.799368	65	0.914	17.846
27	80.5	clay	0.412	0.143556	1.47	2.241585	80.5	0.914	25.969
28	30.8	sand	0.072	0.015046	2.34	1.283442	30.8	1.524	9.538
29	31.5	clay	0.3	0.062691	2.13	1.168261	31.5	1.524	9.846
30	40	silt	0.072	0.015046	3.52	1.930648	40	1.524	15.076
31	41.3	clay	0.374	0.078155	2.46	1.34926	41.3	1.524	14.769
32	53.2	silt	0.429	0.089648	2.46	1.34926	53.2	1.524	22.461
33	58	clay	0.582	0.121621	3.28	1.799013	58	1.524	26.461
34	75	clay	0.668	0.139592	4.1	2.248766	75	1.524	42.461
35	110	clay	0.903	0.188701	4.93	2.704004	110	1.524	82.154
36	40	clay	0.306	0.079944	2	1.714561	40	1.219	11.323
37	80.5	clay	0.556	0.145258	2.62	2.246075	80.5	1.219	32.277
38	40	clay	0.229	0.079792	1.12	1.707875	40	0.914	8.123
39	80.5	clay	0.417	0.145298	1.48	2.256834	80.5	0.914	28.184
40	40	clay	0.347	0.090656	2.1	1.800289	40	1.219	11.938
41	80.5	clay	0.589	0.15388	2.93	2.511832	80.5	1.219	79.877
42	40	clay	0.26	0.090594	1.18	1.799368	40	0.914	8.738
43	80.5	clay	0.442	0.154009	1.65	2.516065	80.5	0.914	29.046

2.5. Gene Expression Programming (GEP)

By combining the tenets of genetic programming (GP) and genetic algorithms (GA), Ferreira created gene expression programming [28]. Evaluating more complicated programs made up of multiple subprograms is made possible by the proposed approach's strength—its simplicity in producing genetic diversity—as well as its unique and multi-genic nature. In order to build a computer program that can simulate a given phenomena, GEP as GA uses an approach that is similar to biological evolution. The five components of a GEP algorithm—the function set, the terminal set, the fitness function, the control parameters, and the halting condition—are chosen at the outset. In every step that follows, the projected values are compared to the actual values. We end the GEP process when the previously chosen error criteria produce the expected results. The process ends when the target fitness score is reached, and the optimal solution to the problem is determined by decoding the chromosomes. Here are some of the main benefits of GEP: (1) chromosomes are uncomplicated units of genetic material, and (2) expression trees include just chromosome-specific expression. It is worth mentioning that GeneXproTools 4.0 Release 2 was utilized to build this technique. The GEP modeling method, as shown in Fig. 4, starts with the starting population's chromosomes being generated at random.

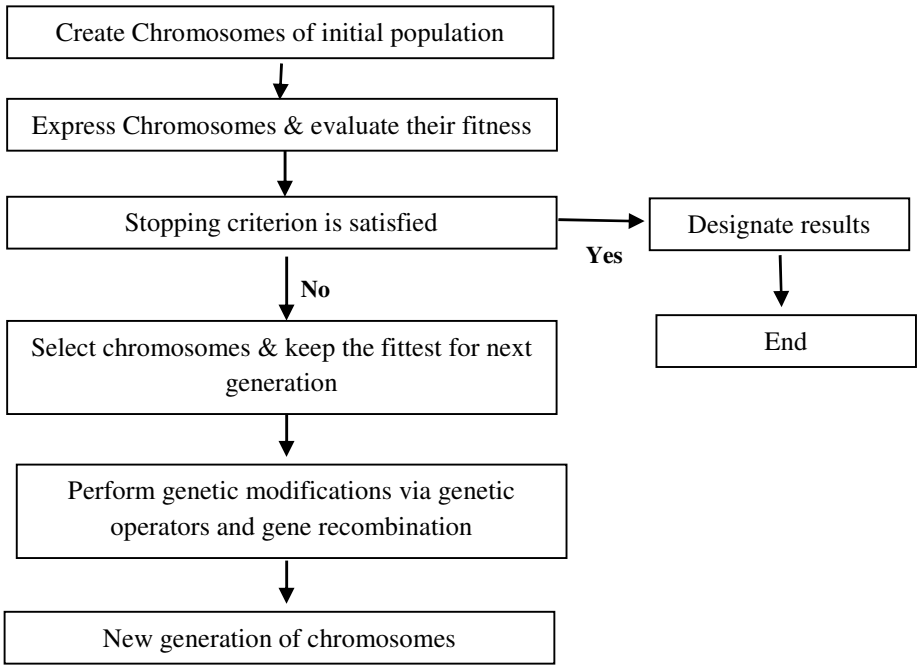

Fig. 1 The flowchart of GEP procedure

3. Development of Gene Expression Programming Models

3.1. Data Division and Models Pre-Processing

Models for analyzing piles' axial bearing capacity using CPT data have been developed in this research utilizing GEP. Soil type is used to categorize the data into cohesive and non-cohesive groupings. Additionally, the database is partitioned into two parts: training data, which comprises 80% of the data, and test data, which comprises 20% of the data, for the purpose of controlling the performance of the models. Table 2 shows the results of the calculations for the maximum, minimum, mean, and standard deviation of the data included in these two groups. These calculations were done in accordance with the principles of data mining in order to generate suitable testing and training databases. It is expected that both subgroups will be statistically representative of the whole population due to the random makeup of the subgroups. The final, approved models can also reliably calculate Qu using both trained and untrained data.

Table 2. Statistical features for training and testing database

	Training Data					Testing Data				
	q_c(MPa	f_s(MPa)	L(m)	D(m)	Q_u(KN)	q_c(MPa)	f_s(MPa)	L(m)	D(m)	Q_u(KN)
Cohesionless soil										
Max	3.08	0.14	100.5	1.524	67719	1.951	0.14001	96	1.524	61248
Min	1.34	0.0148	39.2	0.914	8000	1.283	0.0149	30.8	0.0914	6581
Mean	1.87	0.0486	56.07	1.38	25865.67	1.59	0.0618	51.825	1.3715	22837.5
S.D	0.45	0.049	21.56	0.208	19380.16	0.285	0.051	25.79	0.264	22232.26
Cohesive soil										
Max	2.7	0.188	110.5	1.524	82154	2.516	0.154	84.5	1.524	49461
Min	1.16	0.062	31.5	0.914	6684	1.34	0.078	40	0.914	11323
Mean	1.95	0.12	65.86	1.23	30534.68	1.911	0.117	64.25	1.18	246845
S.D	0.35	0.03	23.42	0.25	23668.8	0.363	0.029	18.79	0.23	12573.69

Following this, GEP was taught to estimate local loss coefficients using a set of mathematical functions (x2, x3) and the basic arithmetic operators (+, -,*, /). Table 3 displays the different chromosomal structure combinations that were tested. After that, the model was run for a few generations before being stopped when the fitness function value and coefficient of correlation did not show any significant changes. Models with 30 chromosomes, 8 genes for head size, and 3 genes for number of copies produced superior outcomes. When getting the GEP model ready, picking the right genetic operators is a crucial first step. Thus, it was also necessary to evaluate a combination of all genetic operators. Table 3 displays the optimized GEP model properties.

Table 3. Optimized parameters of GEP models

parameter	setting
Function set	+, -, ×, /, x^2, x^3, $\sqrt{}$
Chromosomes	25, **30**, 35
Head size	7, **8**
Linking function	addition
Fitness function	Root mean square error

3.2. Models Performance and Robustness

The approaches' efficiency was assessed using statistical measures, such as the root means square error (RMSE) and the correlation coefficient (R). The root-mean-squared error (RMSE) is similarly expressed in terms of kN as the goal parameter (Qu). Here are the correlations between these statistical parameters:

$$R = \frac{\sum_{i=1}^{N}(I_0 - \overline{I_0}) \times (I_P - \overline{I_P})}{\sqrt{\sum_{i=1}^{N}(I_0 - \overline{I_0})^2 \times (I_P - \overline{I_P})^2}} \quad (1)$$

$$RMSE = \sqrt{\sum_{i=1}^{N} \frac{(I_0 - I_P)^2}{N}} \quad (2)$$

The measured values, predicted values, mean measured values, mean predicted values, and number of data samples are represented by I_0,I_P, $\overline{I_0}$, $\overline{I_P}$, N, respectively.

In order to ensure accurate analysis findings, it is important to carefully choose the input models in GEP. By doing so, the parameters used to determine the pile's bearing capacity may be more effectively controlled. Extensive research has shown that the following critical characteristics can influence bearing capacity: pile diameter (D), pile tip resistance (qc), and pile friction resistance (fs).

Section 4: Discussions and Findings

Part 4.1: GEP Models for Development

For cohesive soils, the GEP model expression trees are presented in Fig. 5, and for non-cohesive soils, they are shown in Fig. 6. An advantage of GEP approaches, as previously stated, is that they automatically formulate the link between model inputs and their associated outputs in a

mathematical equation that users can access. Equations 3 for driven piles in cohesive soils and Eq. 4 for non-cohesive soils provide straightforward mathematical formulations of the model expression trees.

$$Q_u = \left(0.64\frac{L}{D^4}\right)(f_s + L) + (3.77 - f_s)^{1.5}({q_c}^3 - D^3)^3 + 38.25L^{1.5}D \quad (3)$$

$$Q_u = -((q_c + 6.12)^3 - q_c L)(q_c - 6.12D + 6.59) + (3.5 - 2L)^2 + (DL(q_c + L) + (7.13D)(L + 7.13)(2.43f_s + 7.13D) \quad (4)$$

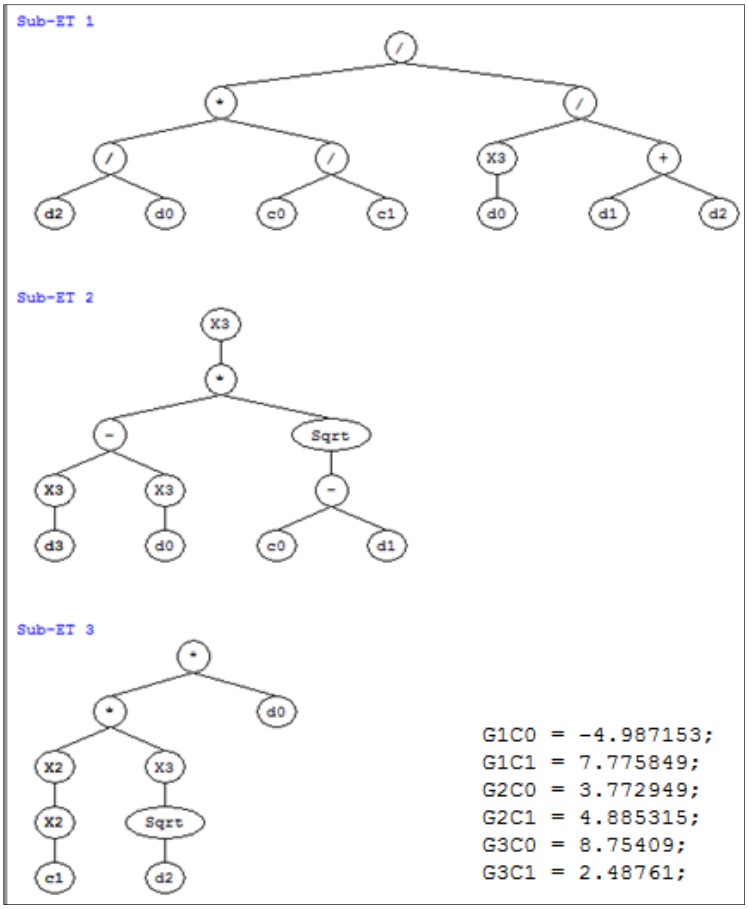

Fig. 5 Expression tree (ET) of the GEP model formulation for driven piles in cohesive soils

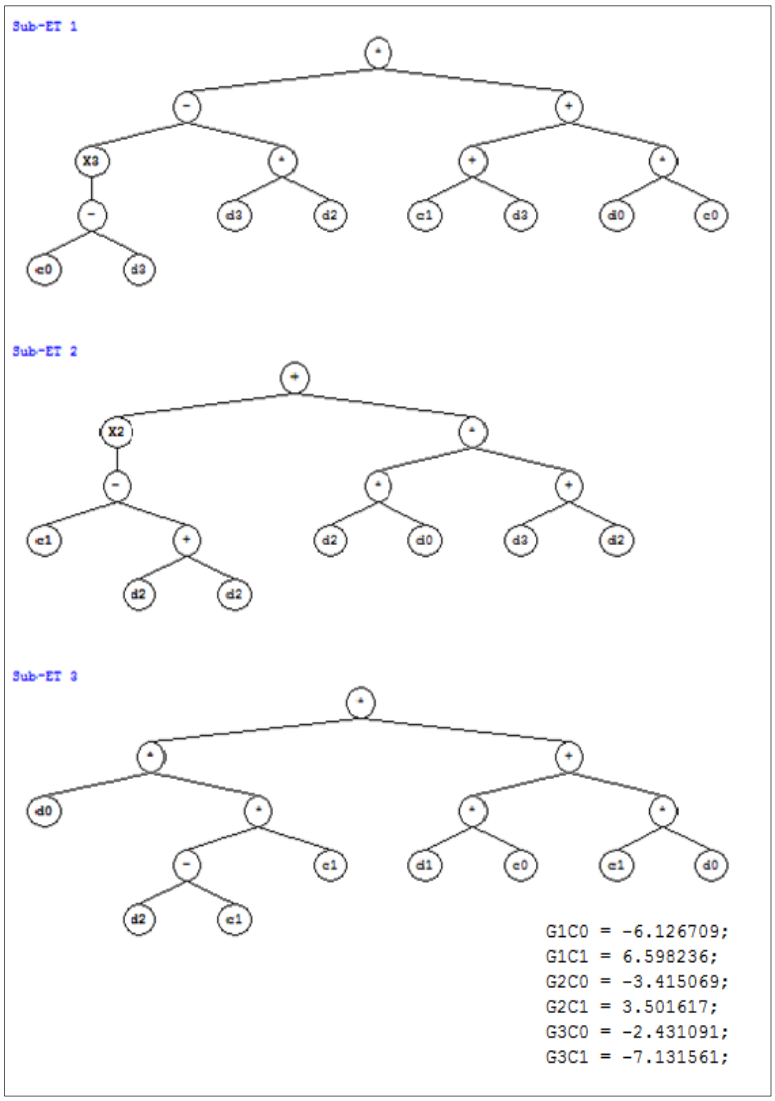

Fig. 6 Expression tree (ET) of the GEP model formulation for driven piles in non-cohesive soils

Both cohesive and non-cohesive soils can have their pile carrying capacity predicted using these models. To calculate the pile's bearing capacity, the model takes into account the pile's diameter and length, the strength of the pile's tips, and the resistance to friction. Presented in Table 4 are the findings from the examination of GEP models. Table 4 shows that there is a good correlation between the data sets, indicating that the cohesive and non-cohesive soils exhibit promising correlation values. Conversely, compared to cohesive soils, non-cohesive soils have higher input data correlation values with the goal function.

Table 3. Statistical parameters of the GEP models

Models	R^2	RMSE	R^2	RMSE
	train		test	
Cohesive soil	0.91	0.071	0.84	0.054
Non-cohesive soil	0.99	0.029	0.98	0.011

Experimental data has been used to validate these models, assessing their correctness and performance. Figures 7 and 8 display the projected Qu values compared to the measured values for cohesive soils in the training data subset, whereas Figures 9 and 10 demonstrate the same for non-cohesive soils. In light of this, the suggested models are able to foretell the pile's final axial bearing capacity. As shown in Figures 7 and 8, the recommended model for cohesive soil has an R2 of 0.91 and an RMSE of 7.1% for the training data, as well as 0.84 and 5.4% for the testing data. The suggested model for non-cohesive soil has an R2 of 0.99 and an RMSE of 2.9% for the training data, as shown in Figures 9 and 10, and these values drop to 0.99 and 1/1% for the testing data, respectively.

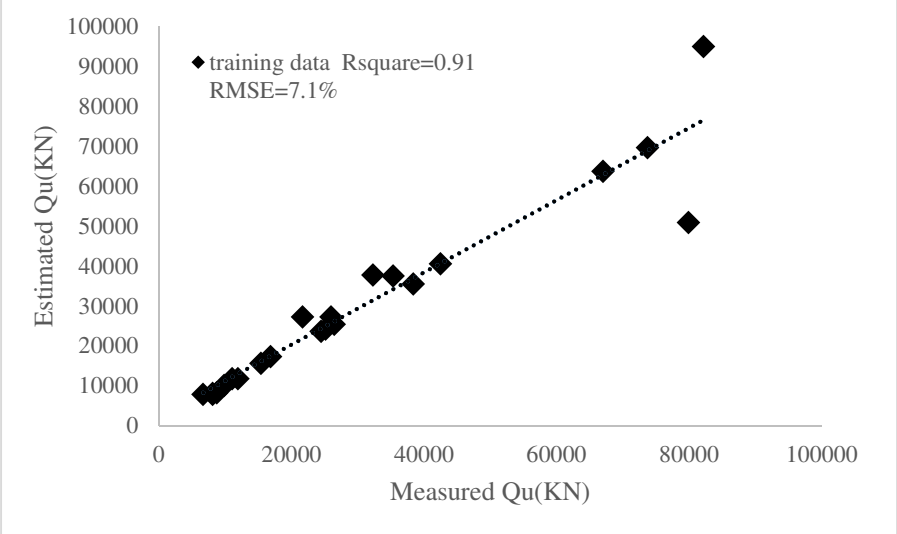

Fig. 7 Performance comparison of GEP driven piles model and CPT based methods in cohesive soils for training data

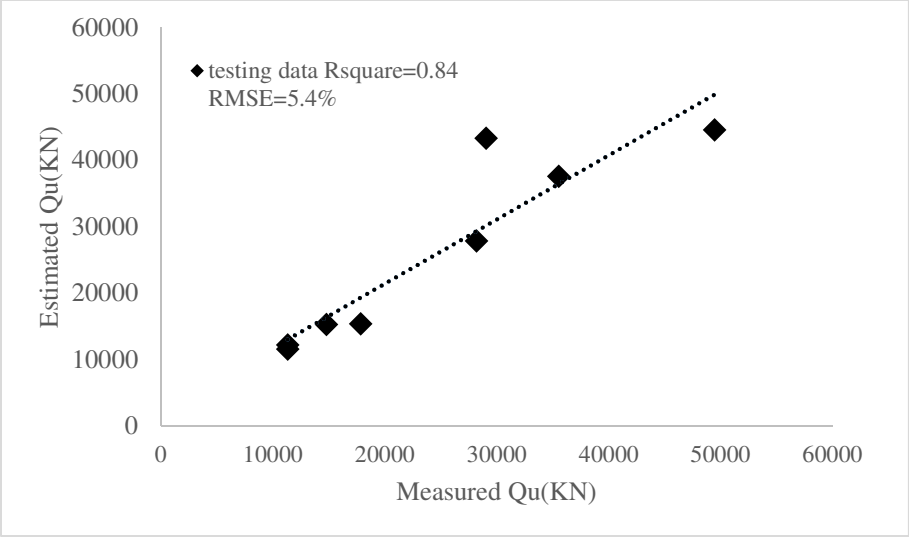

Fig. 8 Performance comparison of GEP driven piles model and CPT based methods in cohesive soils for testing data

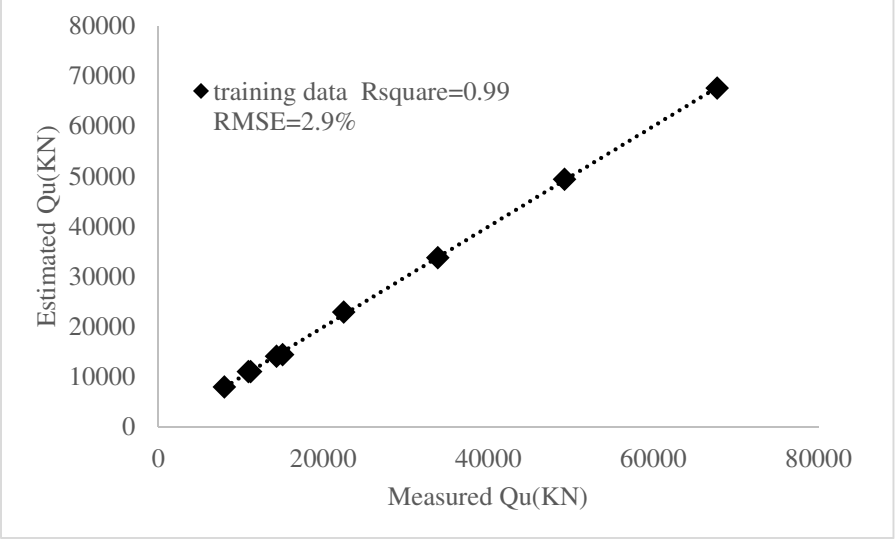

Fig. 9 Performance comparison of GEP driven piles model and CPT based methods in non-cohesive soils for training data

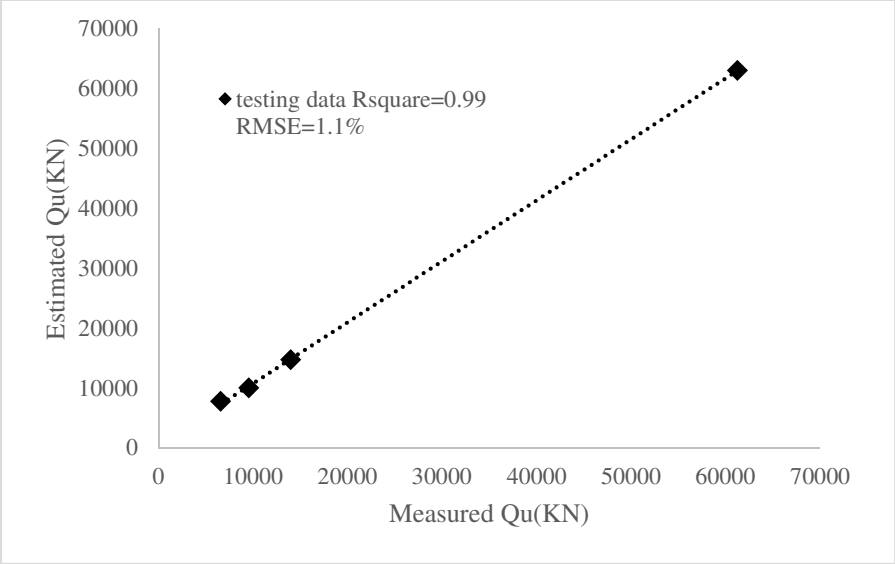

Fig.10 Performance comparison of GEP driven piles model and CPT based methods in non-cohesive soils for testing data

4.2. Calibration Based on PDA Results

We offer an analytical equation that, drawing on previous research, can be used to calculate the compressive axial bearing capacity of tubular metal piles in the Persian Gulf area. Then, we calibrate this relationship using data from PDA field testing. Figures 11–14 show the outcomes of this calibrating method. Figures 11 and 12 in the case of cohesive soils and Figures 13 and 14 in the case of non-cohesive soils show the projected values of Qu compared to the measured values for the training and test data subset, respectively, after calibration. In light of this, the suggested models are able to foretell the pile's final axial bearing capacity. As shown in Figures 11 and 12, the recommended model for cohesive soils has an R2 value of 0.91 and an RMSE of 1.2% for the training data, as well as 0.92 and 1.25% for the testing data. Be. The suggested model for non-cohesive soils has an R2 of 0.99 and an RMSE of 1.9% for training data, as well as 0.99 and 1% for testing data, respectively (see Figs. 13 and 14).

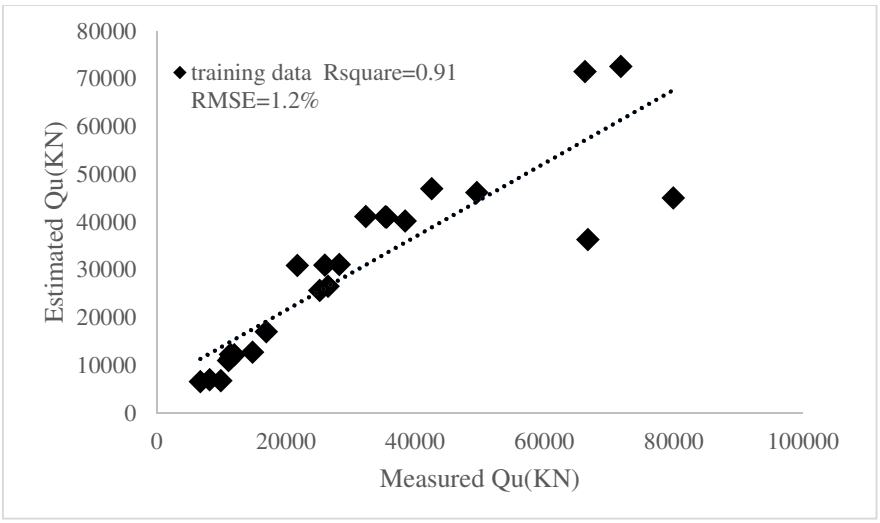

Fig. 2 Calibration Performance comparison of GEP driven piles model and PDA based methods in cohesive soils for training data

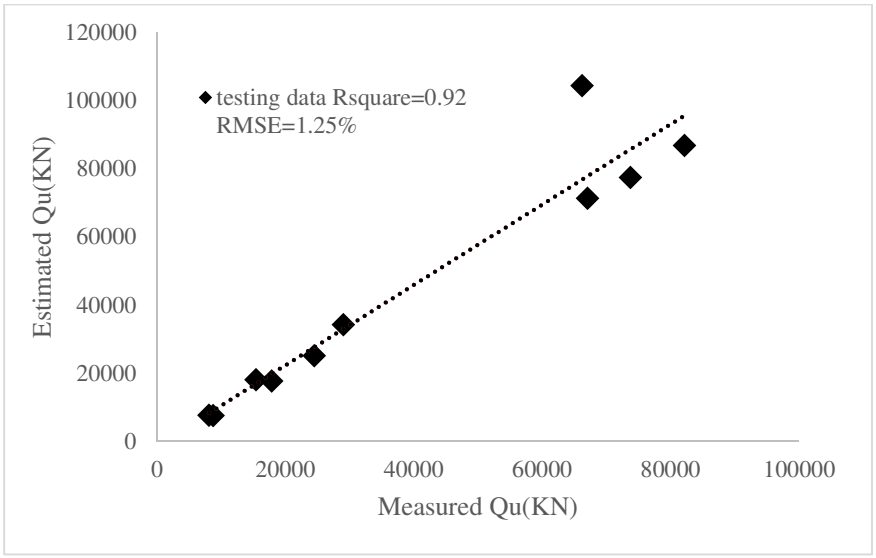

Fig. 3 Calibration Performance comparison of GEP driven piles model and PDA based methods in cohesive soils for testing data

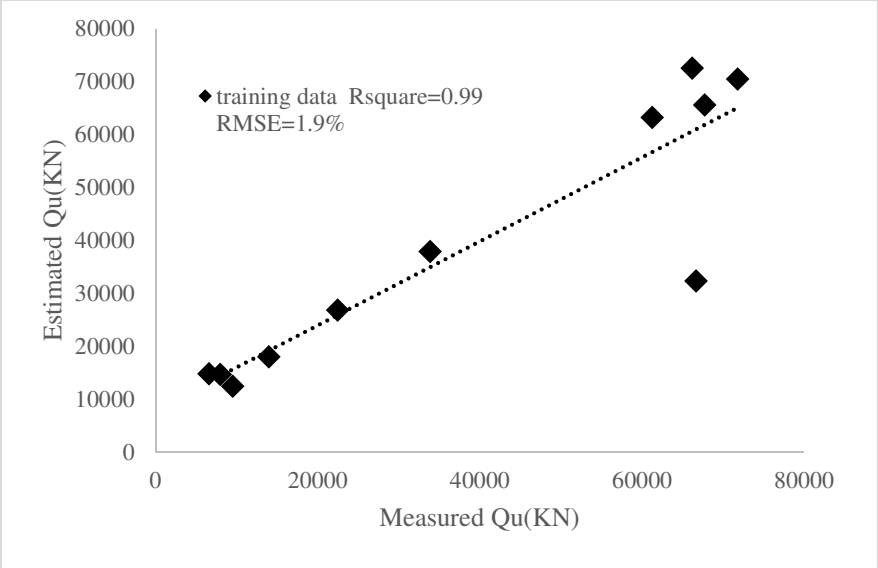

Fig. 4 Calibration Performance comparison of GEP driven piles model and PDA based methods in non-cohesive soils for training data

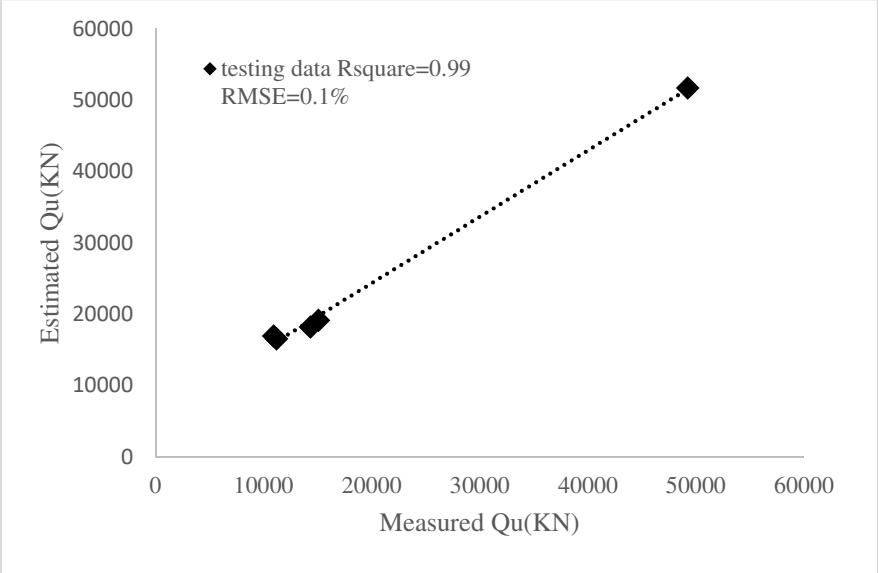

Fig. 5 Calibration Performance comparison of GEP driven piles model and PDA based methods in non-cohesive soils for testing data

4.3. Optimization the Dimensions of Driven Piles

In order to train the model using a series of randomized input-output pairs, the GEP must first be used in optimization as a quick analyzer. It is necessary to regulate the model's execution in order to maintain an appropriate level of output accuracy. With the network trained and in structural optimization, reanalysis of the structure is unnecessary; however, the GEP serves as a quick analyzer during the many iterations. Aiming for optimal pile length and diameter was the focus of the current investigation. Optimization plots are displayed in the following figures for this purpose. For various values of fs and qc, the optimal ratio of length to pile diameter is around 40, as demonstrated in Figures 15–19, when the ratio falls between 19 and 75.

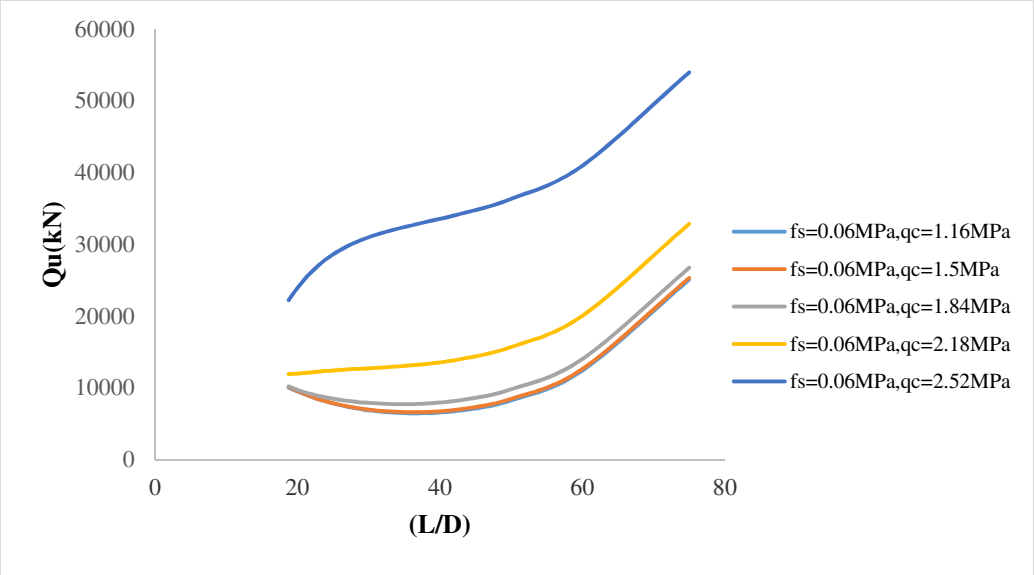

Figure 6 Optimal values of length to diameter ratio of piles for fs = 0.06MPa and different values of qc

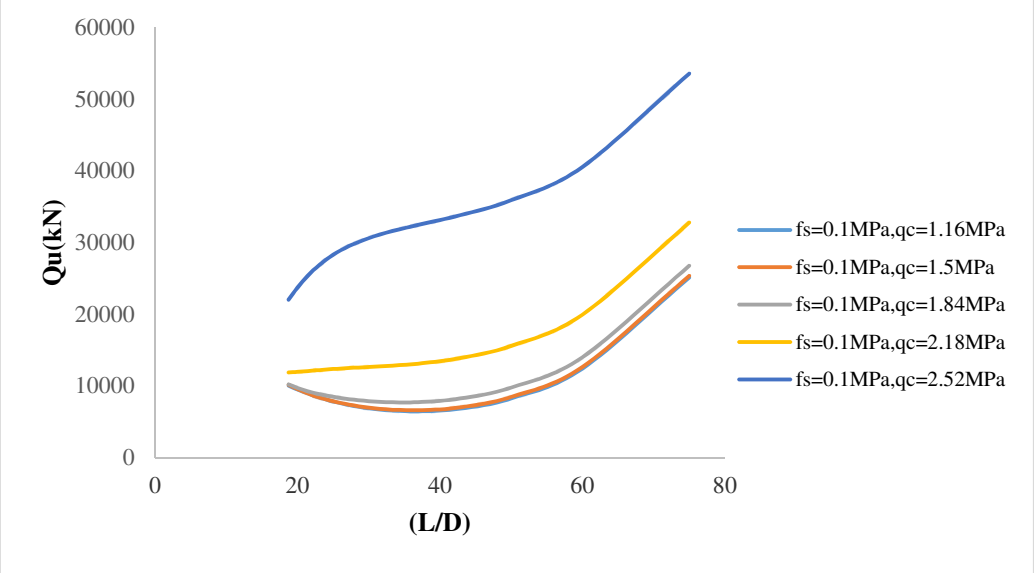

Fig. 7 Optimal values of length to diameter ratio of piles for fs = 0.1MPa and different values of qc

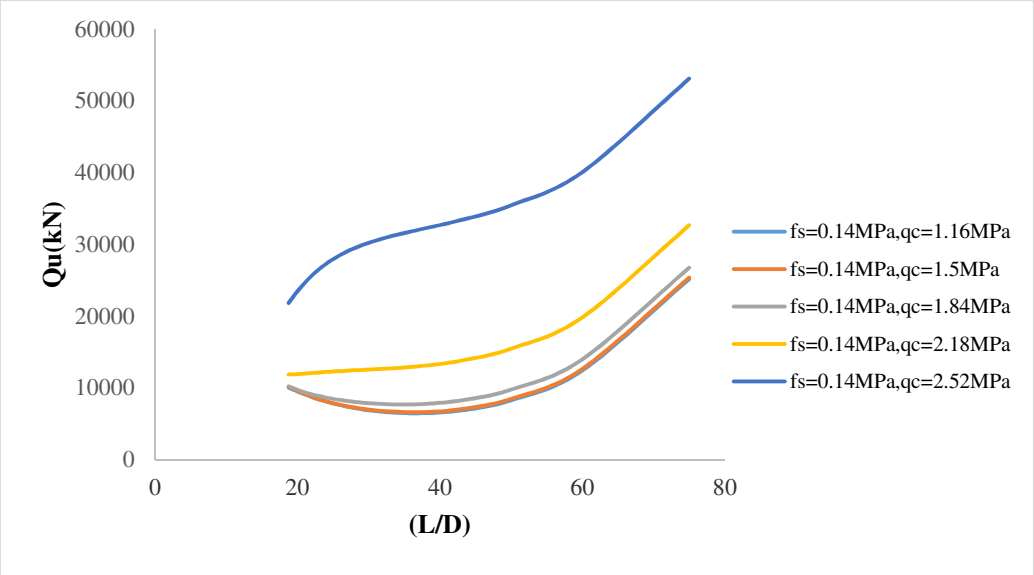

Fig. 8 Optimal values of length to diameter ratio of piles for fs = 0.14MPa and different values of qc

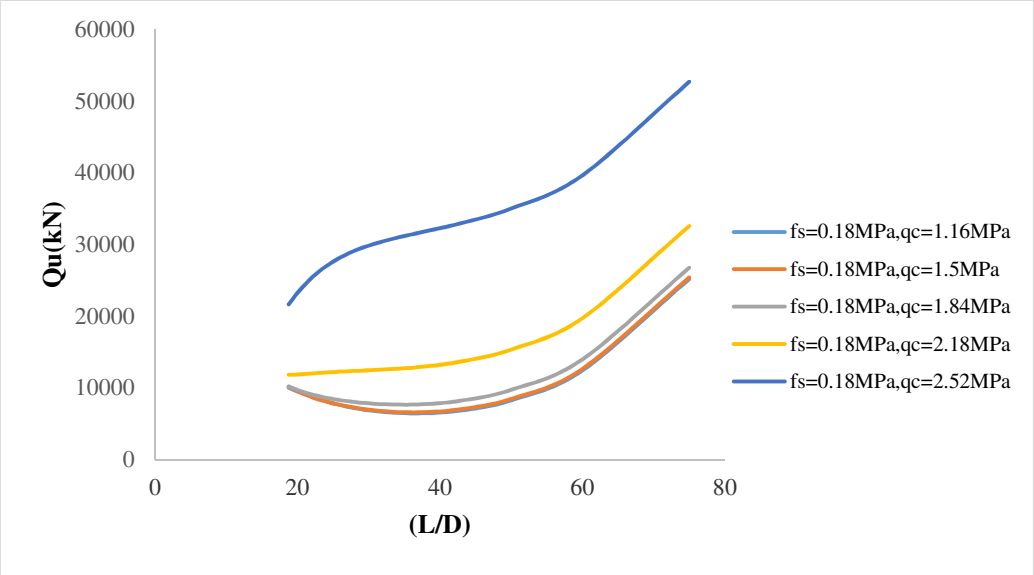

Fig. 9 Optimal values of length to diameter ratio of piles for fs = 0.18MPa and different values of qc

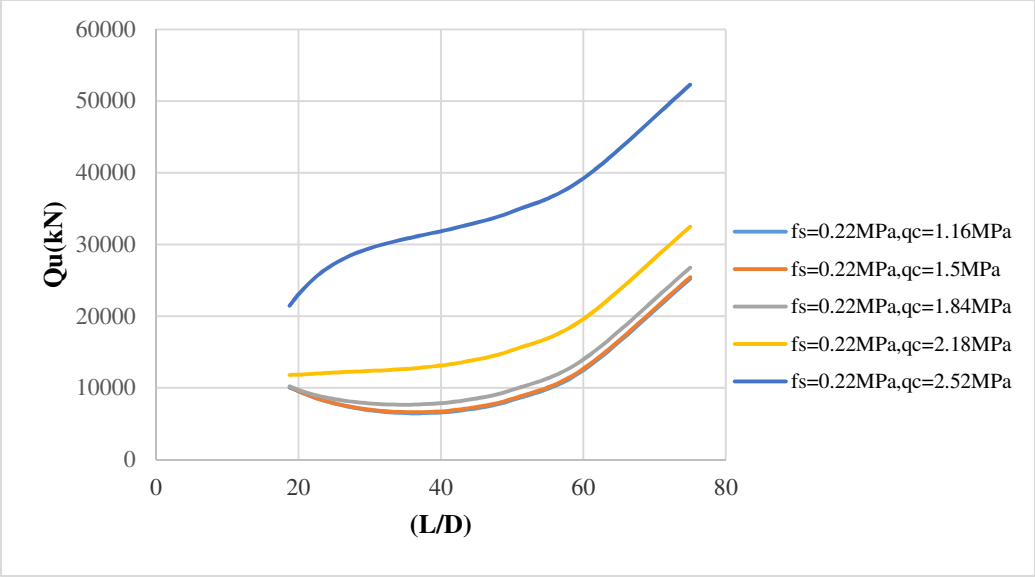

Fig. 10 Optimal values of length to diameter ratio of piles for fs = 0.22MPa and different values of qc

5. Conclusions

Findings from the computational study of the GEP model and the CPT were used to ascertain the bearing capacity of offshore steel pipe piles driven in the Persian Gulf (South Pars). The outcomes of the piles dynamic tests (PDA) were used to calibrate the GEP models. Based on the current data and calibration, the optimized pile dimensions were also computed. Axial bearing capacity of piles evaluated with GEP and CPT data has been developed. Pile diameter (D), pile tip resistance (qc), friction pile resistance (fs), and pile length (L) are effective factors that determine the ultimate loading capacity of the pile. Soil cohesiveness and non-cohesiveness were initially defined as part of this study's framework. After that, models were created to forecast how much weight piles in cohesive and non-cohesive soils might support. In this instance, the models use the pile's diameter and length, as well as its friction resistance, tip strength, and bearing capacity to make their predictions. Positive findings from the correlation values in cohesive and non-cohesive soils indicate that the data are highly connected. The recommended model for cohesive soil has an R2 of 0.91 and an RMSE of 7.1% for the training data, as well as 0.84 and 5.4% for the testing data. Moreover, the suggested model for non-cohesive soil has an R2 of 0.99 and an RMSE of 2.9% for the training data, as well as 0.99 and 1.1% for the testing data. The suggested model for cohesive soil shows an R2 value of 0.92 and an RMSE value of 1.25% for training data after calibration using PDA findings; for testing data, the corresponding values are 0.91 and1.2%, respectively. R2 for training data is 0.99 and RMSE for testing data is 1, respectively, as a consequence of PDA calibration in the suggested model for non-cohesive soil. The results demonstrate that, for various fs and qc, a length-to-diameter ratio of approximately 40 is best, with a range of 19–75.

References

[1] Speight, J.G., 2014. *Handbook of offshore oil and gas operations*. Elsevier.

[2] Wahab, M.M.A., Kurian, V.J., Liew, M.S. and Kim, D.K., 2020. Condition assessment techniques for aged fixed-type offshore platforms considering decommissioning: A historical review. *Journal of Marine Science and Application*, *19*(4), pp.584-614.

[3] Reddy, D.V. and Swamidas, A.S.J., 2013. *Essentials of offshore structures: framed and gravity platforms*. CRC press.

[4] Chandrasekaran, S. and Jain, A., 2017. *Ocean structures: Construction, materials, and operations*. Crc Press.

[5] Sani, A.H.A., Husain, M.A., Zaki, N.M., Mukhlas, N.A. and Ahmad, S.S., 2021. Effect of pile scouring on structural integrity of fixed offshore jacket structures. *Journal of Advanced Research in Applied Mechanics*, *86*(1), pp.1-11.

[6] Stahlmann, A. and Schlurmann, T., 2010. Physical modeling of scour around tripod foundation structures for offshore wind energy converters. In *Proceedings of the Coastal Engineering Conference (2010)*. Reston: American Society of Civil Engineers.

[7] Eslami, A., Aflaki, E. and Hosseini, B., 2011. Evaluating CPT and CPTu based pile bearing capacity estimation methods using Urmiyeh Lake Causeway piling records. *Scientia Iranica*, *18*(5), pp.1009-1019.

[8] Adel, R. and Shakir, R.R., 2022. Evaluation of Static Pile Load Test Results of Ultimate Bearing Capacity by Interpreting Methods. In *IOP Conference Series: Earth and Environmental Science* (Vol. 961, No. 1, p. 012013). IOP Publishing.

[9] Yu, Y.W., 2009. Pile driving analysis via dynamic loading test.

[10] Zhussupbekov, A.Z., Omarov, A.R. and Kaliakin, V.N., 2019. Prediction of axial bearing capacity of piles by SPT and PMT-based approach. In *Geotechnics Fundamentals and Applications in Construction: New Materials, Structures, Technologies and Calculations* (pp. 435-440). CRC Press.

[11] Karkush, M.O., Sabaa, M.R., Salman, A.D. and Al-Rumaithi, A., 2022. Prediction of bearing capacity of driven piles for Basrah governatore using SPT and MATLAB. *Journal of the Mechanical Behavior of Materials*, *31*(1), pp.39-51.

[12] Wei, Y., Wang, D., Li, J., Jie, Y., Ke, Z., Li, J. and Wong, T., 2020. Evaluation of ultimate bearing capacity of pre-stressed high-strength concrete pipe pile embedded in saturated sandy soil based on in-situ test. *Applied Sciences*, *10*(18), p.6269.

[13] Cai, G., Liu, S., Tong, L. and Du, G., 2009. Assessment of direct CPT and CPTU methods for predicting the ultimate bearing capacity of single piles. *Engineering Geology*, *104*(3-4), pp.211-222.

[14] Gwizdala, K., 1984. *Large diameter bored piles in non-cohesive soils. Determination of the bearing capacity and settlement from results of static penetration tests (CPT) and standard penetration test (SPT)*.

[15] Eslami, A. and Fellenius, B.H., 1995, October. Toe bearing capacity of piles from cone penetration test (CPT) data. In *Proceedings of the International Symposium on Cone Penetration Testing, CPT* (Vol. 95, pp. 4-5).

[16] Eslami, A. and Fellenius, B.H., 1997. Pile capacity by direct CPT and CPTu methods applied to 102 case histories. *Canadian Geotechnical Journal*, *34*(6), pp.886-904.

[17] Titi, H.H. and Abu-Farsakh, M.Y., 1999. Evaluation of Bearing Capacity of Piles from Cone Penetration Test Data [1999].

[18] Gwizdała, K. and Stięczniewski, M., 2007. DETERMINATION OF THE BEARING CAPACITY OF PILE FOUNDATIONS BASED ON CPT TEST RESULTS. *Studia Geotechnica et Mechanica*, *29*.

[19] Cai, G., Liu, S. and Puppala, A.J., 2011. Evaluation of pile bearing capacity from piezocone penetration test data in soft Jiangsu Quaternary clay deposits. *Marine georesources & geotechnology*, *29*(3), pp.177-201.

[21] Moshfeghi, S. and Eslami, A., 2018. Study on pile ultimate capacity criteria and CPT-based direct methods. *International Journal of Geotechnical Engineering*, *12*(1), pp.28-39.

[21] Alkroosh, I. and Nikraz, H., 2011. Correlation of pile axial capacity and CPT data using gene expression programming. *Geotechnical and Geological Engineering*, *29*(5), pp.725-748.

[22] API (American Petroleum Institute), 2011. Geotechnical and foundation design considerations. *API RP 2GEO*.

[23] Eslami, A., Moshfeghi, S., Molaabasi, H. and Eslami, M.M., 2019. *Piezocone and cone penetration test (CPTu and CPT) applications in foundation engineering*. Butterworth-Heinemann.

[24] ISSMGE, I., 1999. International reference test procedure for the cone penetration test (CPT) and the cone penetration test with pore pressure (CPTU). *Report of the ISSMGE Technical Committee*, *16*.

[25] Fakharian, K., 2000, May. A Case Study On the Application of Pile Driving Analyzer (PDA) And CAPWAP Analysis to Bearing Capacity of Piles. In *The Tenth International Offshore and Polar Engineering Conference*. OnePetro.

[26] Simanjuntak, J.O. and Suita, D., 2017, December. Analysis of bearing capacity pile foundation with using CAPWAP software for testing pile driving analyzer (PDA) at Fasfel Development Project Parlimbungan Ketek Sikara-Kara Mandailing Natal District (North Sumatera). In *Journal of Physics: Conference Series* (Vol. 930, No. 1, p. 012010). IOP Publishing.

[27] Maizir, H. and Suryanita, R., 2018. Evaluation of axial pile bearing capacity based on pile driving analyzer (PDA) test using Neural Network. In *IOP Conference Series: Earth and Environmental Science* (Vol. 106, No. 1, p. 012037). IOP Publishing.

[28] Ferreira, C., 2001. Gene expression programming: a new adaptive algorithm for solving problems. *arXiv preprint cs/0102027*.